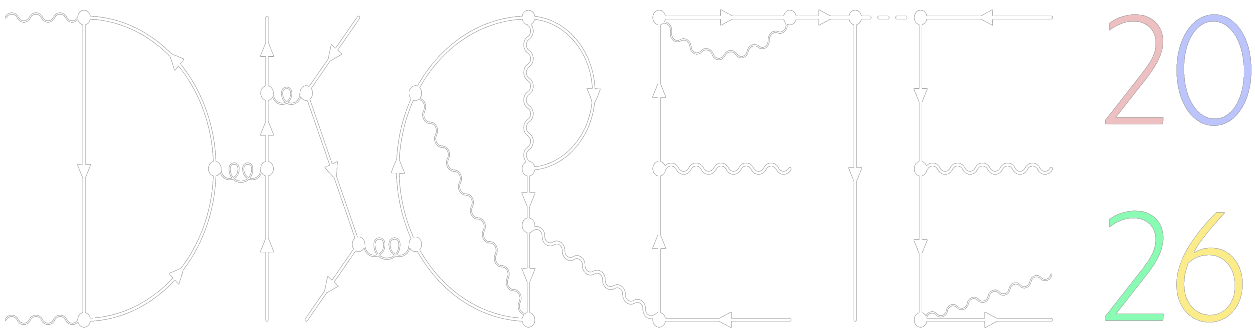
Atomic effects in low-Q nuclear weak decays for direct neutrino-mass measurements

Ovidiu Nițescu

Horia Hulubei National Institute for R&D in Physics and Nuclear Engineering

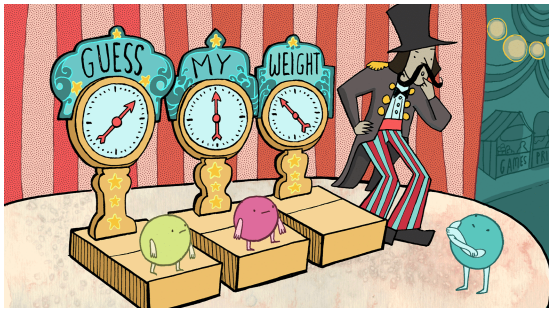
In collaboration with R. Dvornický and F. Šimkovic
Comenius University in Bratislava

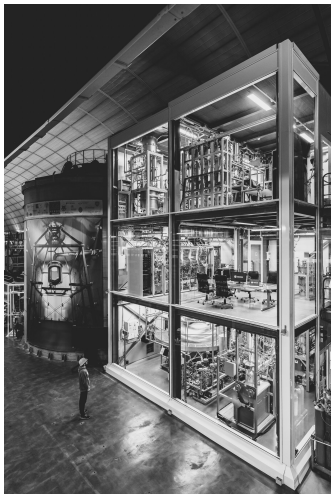


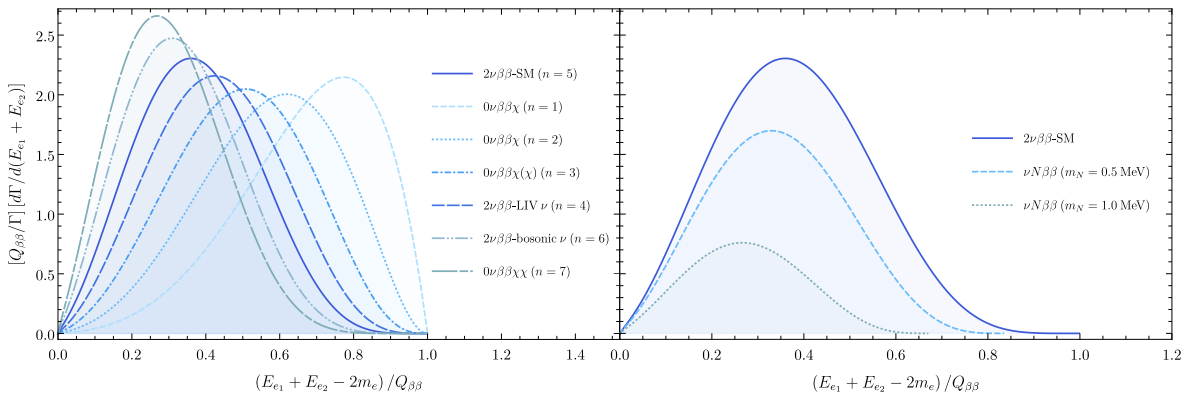
Why precise β and EC theoretical predictions?

The theoretical predictions are required in:

- neutrino mass scale determination from (ultra-)low Q value β and EC transitions (KATRIN, Project-8, ECHo, HOLMES, PTOLEMY) and from $0\nu\beta\beta$ decay
- dark matter searches as they are unavoidable background sources in liquid xenon/argon experiments (XENON, LUX-ZEPLIN, PandaX, XMASS, DarkSide)
- constraining BSM parameters from the shape of β and $\beta\beta$ spectra (most DBD experiments)

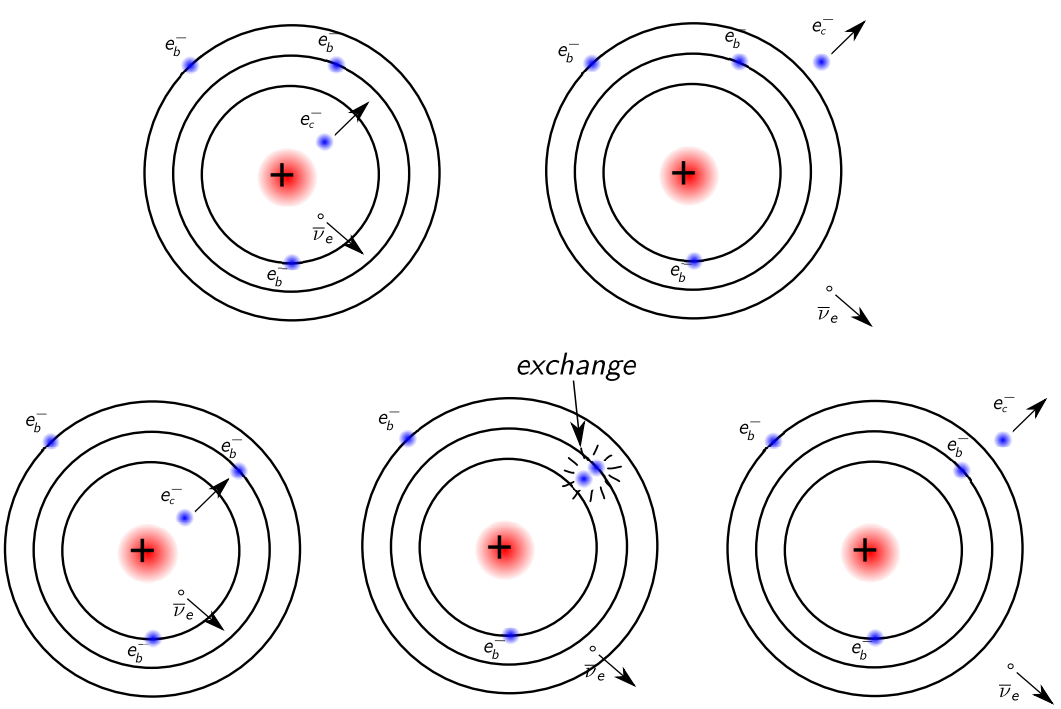






F. Šimkovic, O. Nițescu and J. D. Vergados, Double-beta decay, Encyclopedia of Particle Physics (2026)

Atomic exchange in β^- decay



The observed continuum electron receives contributions from two amplitudes:

- Direct creation in the continuum.
- Creation in a bound orbital, with an initially bound electron emitted.

The amplitudes interfere because electrons are indistinguishable.

$$\frac{d\Gamma}{dE_e} \Rightarrow \frac{d\Gamma}{dE_e} \times \left[1 + \eta^T(E_e)\right]$$

$$\eta^T(E_e) = f_s\,(2T_s + T_s^2) + (1 - f_s)\,(2T_{\bar{p}} + T_{\bar{p}}^2) = \eta_s(E_e) + \eta_{\bar{p}}(E_e)$$

$$T_s = \sum_{(ns)} T_{ns} = -\sum_{(ns)} \frac{\left\langle \psi^f_{E_e s} \middle| \psi^i_{ns} \right\rangle}{\left\langle \psi^f_{ns} \middle| \psi^i_{ns} \right\rangle} \frac{g_{n,-1}(R)}{g_{-1}(E_e, R)}, \qquad f_s = \frac{g^2_{-1}(E_e, R)}{g^2_{-1}(E_e, R) + f^2_{+1}(E_e, R)}.$$

Exchange correction calculation

The overlap between final continuum and initial bound states,

$$\left\langle \psi^f_{E_e\kappa} \middle| \psi^i_{n\kappa} \right\rangle = \int_0^\infty r^2 \left[g^f_\kappa(E_e, r) g^i_{n\kappa}(r) + f^f_\kappa(E_e, r) f^i_{n\kappa}(r) \right] dr.$$

- good knowledge of the continuum w.f. over large distances
- integration method
- orthogonal continuum and bound w.f. for the same atomic system

Phys. Rev. A ***45***, *6282 (1992)*

$$\left\langle \psi^f_{E_e\kappa} \middle| \psi^f_{n\kappa} \right\rangle = 0$$

Standard calculations (true DHFS)

$|\psi_{n\kappa}\rangle$: $V_{\text{nuc}}(r) + V_{\text{el}}(r) + V_{\text{ex}}(r)$

$\left|\psi_{E_e s}\right\rangle$: $V_{\text{nuc}}(r) + V_{\text{el}}(r)$

Phys. Rev. A ***90***, *012501 (2014)*
Rev. Mod. Phys. ***90***, *015008 (2018)*
Phys. Rev. C ***102***, *065501 (2020)*
Phys. Rev. D ***102***, *072004 (2020)*
Appl. Radiat. Isot. ***185***, *110237 (2022)*

Our calculations (modified DHFS)

$|\psi_{n\kappa}\rangle$ and $\left|\psi_{E_e s}\right\rangle$:

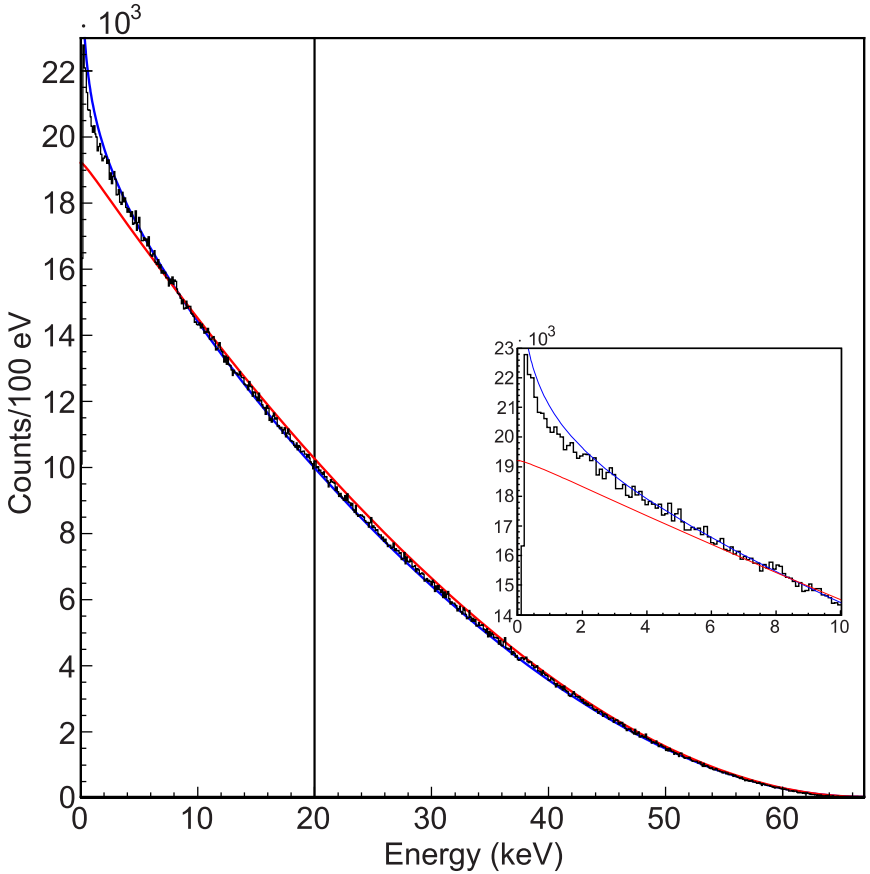
$V_{\text{nuc}}(r) + V_{\text{el}}(r) + V^{\text{Slater}}_{\text{ex}}(r)$

O. Nițescu, S. Stoica and F. Šimkovic Phys. Rev. C ***107***, *025501 (2023)*

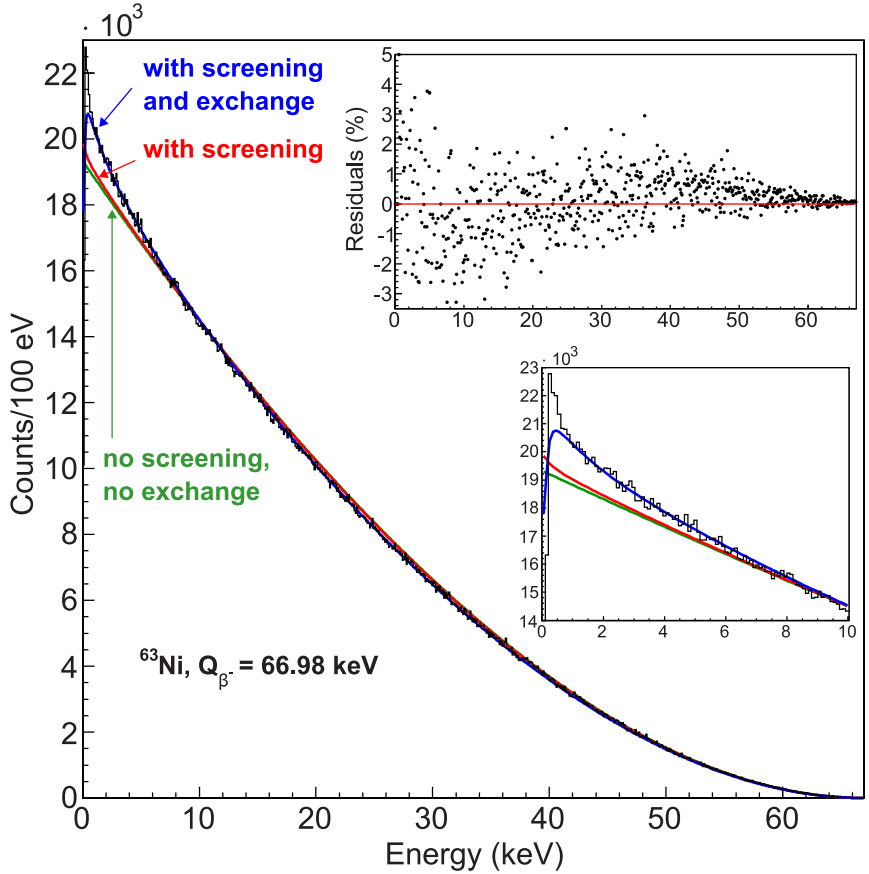
Experimental validation: ^{63}Ni

$$^{63}\mathrm{Ni} \longrightarrow {}^{63}\mathrm{Cu}^{+} + e^{-} + \bar{\nu}_e \qquad Q_\beta = 66.945 \text{ keV}$$

our result: *Phys. Rev. C* ***107***, *025501 (2023)*

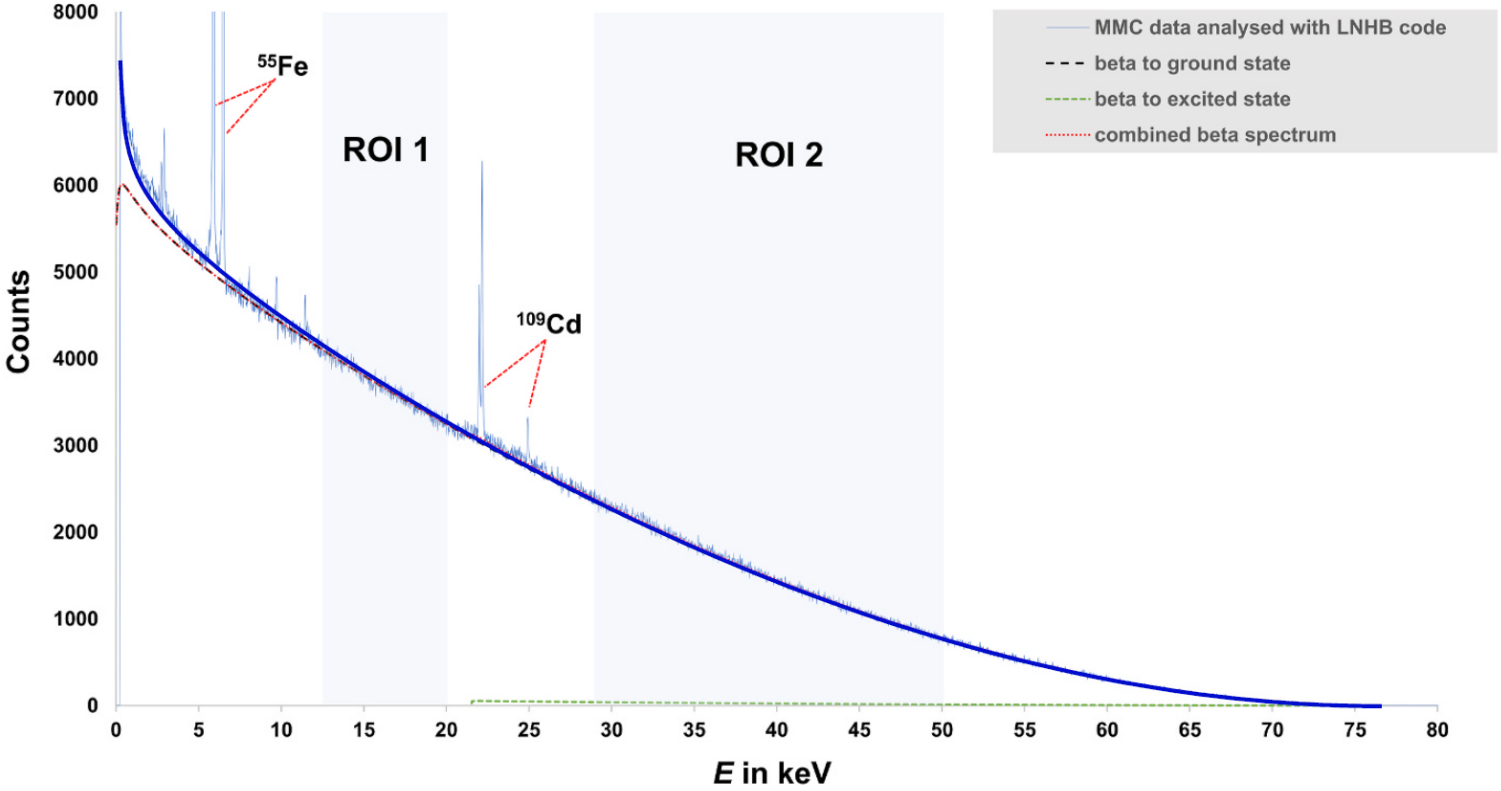


Phys. Rev. A ***90***, *012501 (2014)*



Experimental validation: ^{151}Sm

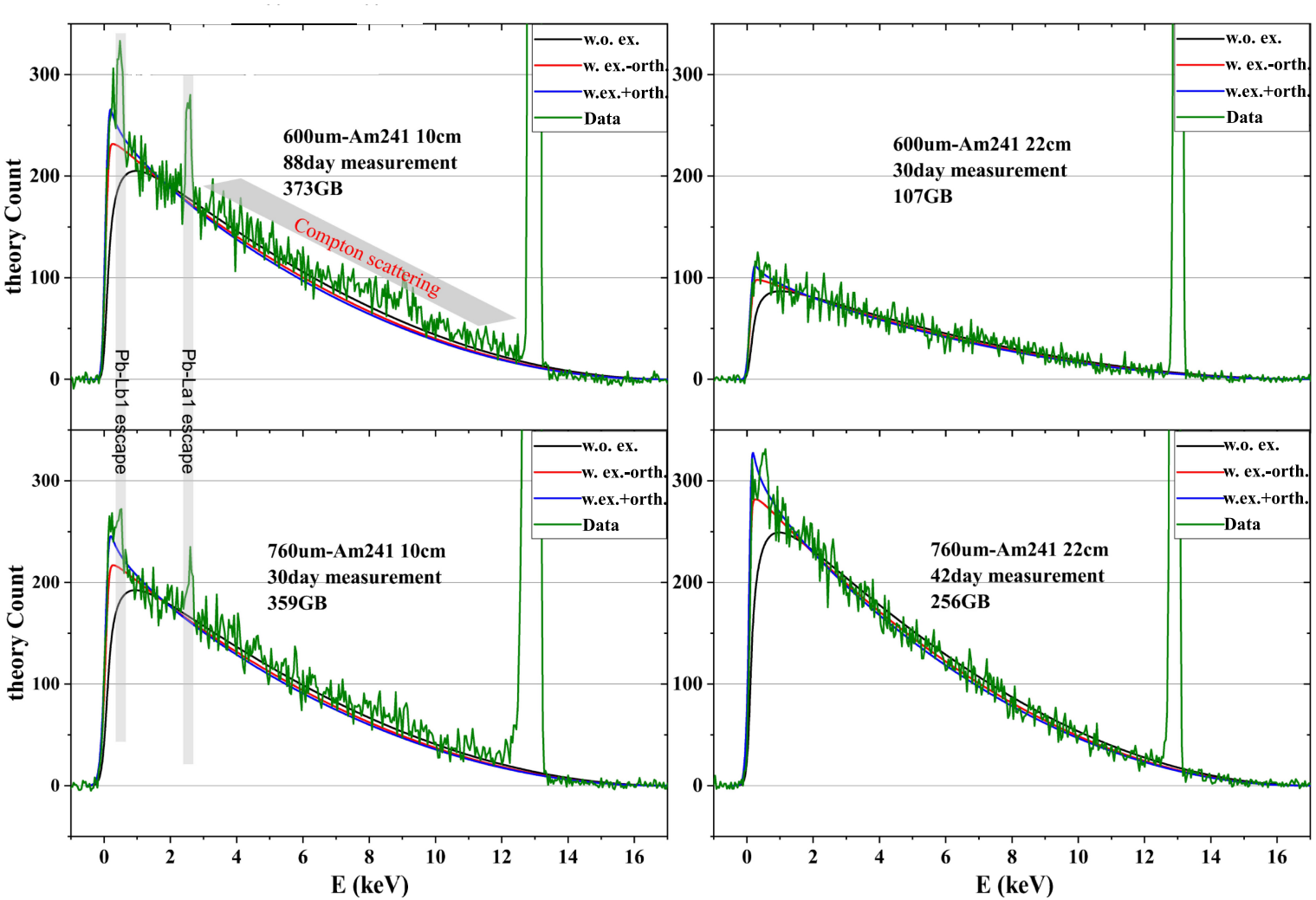
$$^{151}\mathrm{Sm} \longrightarrow {}^{151}\mathrm{Eu}^{+} + e^{-} + \bar{\nu}_e \qquad Q_\beta = 76.6 \text{ keV}$$



Appl. Radiat. Isot. ***185****, 110237 (2022)*

Experimental validation: ^{210}Pb

$$^{210}\mathrm{Pb} \longrightarrow {}^{210}\mathrm{Bi}^{*} + e^{-} + \bar{\nu}_e \qquad Q^{*}_{\beta} = 16.96 \text{ keV}$$



arXiv:2307.16276 (2023)

Enforcing orthogonality largely resolves this discrepancy.

^{187}Re: partial-wave contributions

$$^{187}\mathrm{Re}(5/2^+) \longrightarrow {}^{187}\mathrm{Os}(1/2^-) + e^- + \bar{\nu}_e \qquad Q_\beta = 2.4709\ \mathrm{keV}$$

$$\Gamma = \Gamma_{p_{3/2}} + \Gamma_{s_{1/2}}, \qquad \frac{\Gamma_{p_{3/2}}}{\Gamma_{s_{1/2}}} \simeq 10^4.$$

The unique first-forbidden transition has two partial-wave contributions.

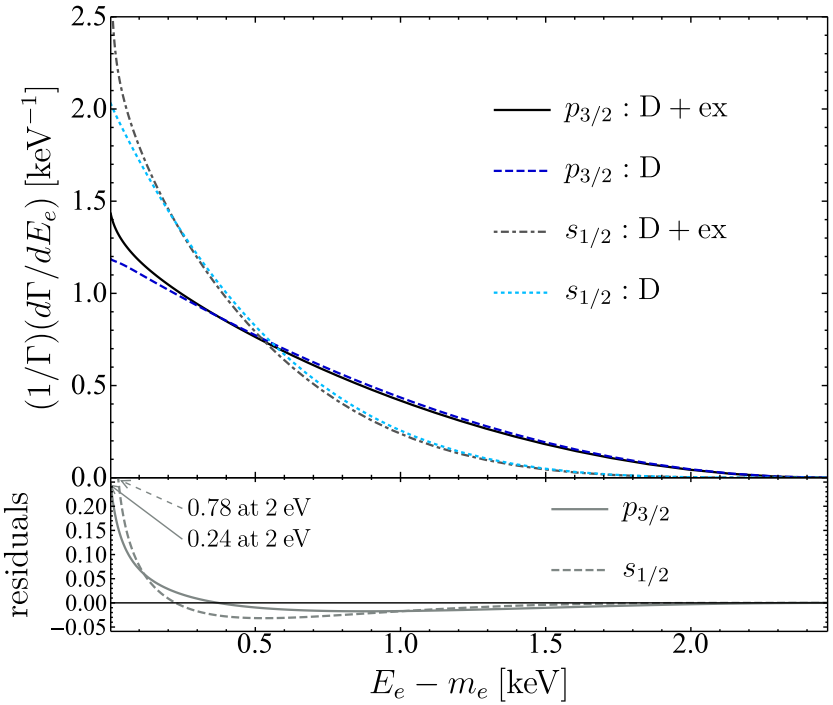
Electron wave functions	Γ_s/Γ_s^A	Γ_p/Γ_p^A
A: approximate	1.000	1.000
D: self-consistent DHFS	0.815	0.760
D with atomic exchange	1.017	0.862

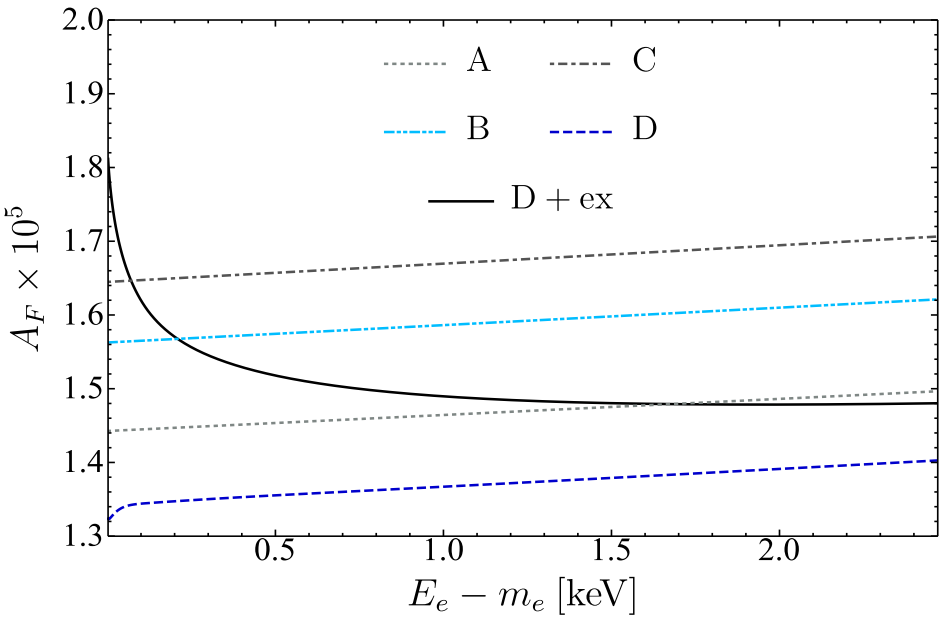
Exchange modifies both rates while $p_{3/2}$ emission remains dominant.

Ratios use the same NME. D includes exact wave functions, a diffuse nuclear charge distribution and screening.

*O. Nițescu, R. Dvornický and F. Šimkovic, Phys. Rev. C **109**, 025501 (2024)*

^{187}Re: spectrum and shape factor





Exchange changes the spectral shape as well as the decay rate.

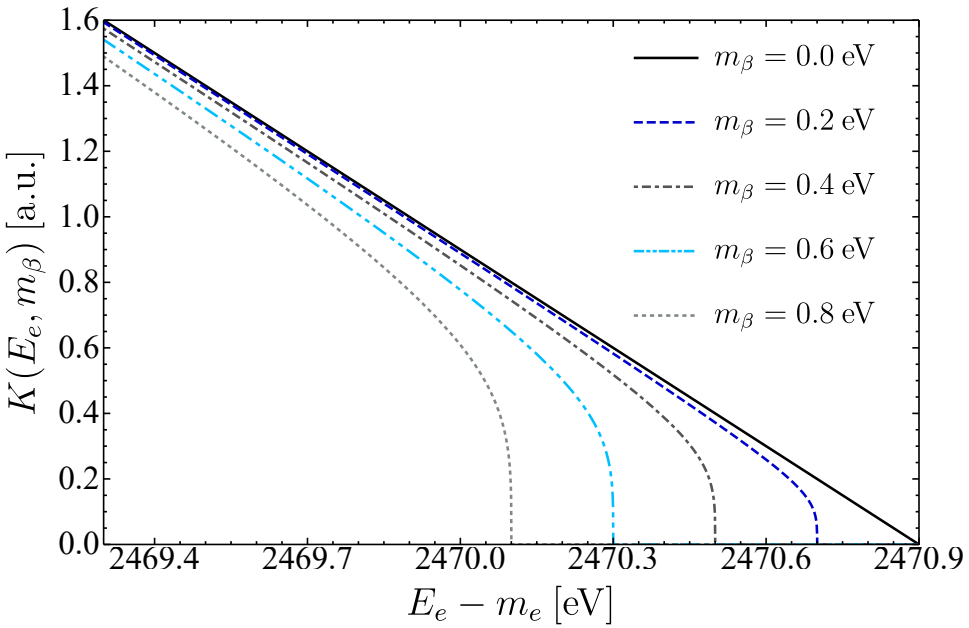
D: self-consistent DHFS; D+ex: DHFS with atomic exchange.

*O. Nițescu, R. Dvornický and F. Šimkovic, Phys. Rev. C **109**, 025501 (2024)*

^{187}Re: exchange in the Kurie plot definition

$$K_{\mathrm{corr}}(E_e, m_\beta) = \sqrt{\frac{d\Gamma/dE_e}{p_e E_e (p_e R)^2 F_1(Z, E_e)\boxed{\left[1+\eta_2^{\mathrm{T}}(E_e)\right]}}}$$

$$= G_F V_{ud}\sqrt{\frac{B}{6\pi^3}}(E_0 - E_e)\sqrt[4]{1-\frac{m_\beta^2}{(E_0-E_e)^2}}\left\{1+\frac{p_\nu^2}{p_e^2}\frac{F_0(Z,E_e)}{F_1(Z,E_e)}\frac{\left[1+\eta_1^{\mathrm{T}}(E_e)\right]}{\left[1+\eta_2^{\mathrm{T}}(E_e)\right]}\right\}^{1/2}$$



Omitting the exchange factor gives

$$K_{\mathrm{omit\,ex}} = \sqrt{1+\eta_2^{\mathrm{T}}(E_e)}\,K_{\mathrm{corr}}.$$

Its energy dependence introduces curvature.

For $m_\beta = 0$, near the endpoint,

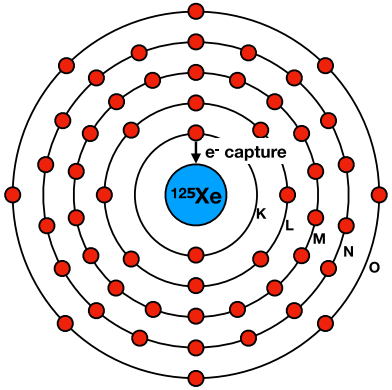
$$K_{\mathrm{corr}} \simeq \mathscr{C}(E_0 - E_e).$$

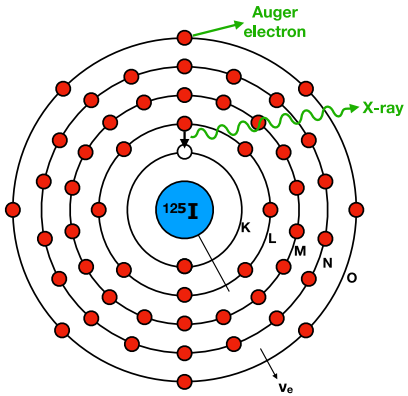
Exchange in the definition preserves massless linearity near the endpoint.

Dominant $p_{3/2}$ channel; the full expression also includes the small $s_{1/2}$ contribution.

*O. Nițescu, R. Dvornický and F. Šimkovic, Phys. Rev. C **109**, 025501 (2024)*

EC to excited states: candidate energies





$$Q^*_{\mathrm{EC}} = Q_{\mathrm{gs}} - E^*, \qquad \Delta_x = Q^*_{\mathrm{EC}} - \varepsilon_x$$

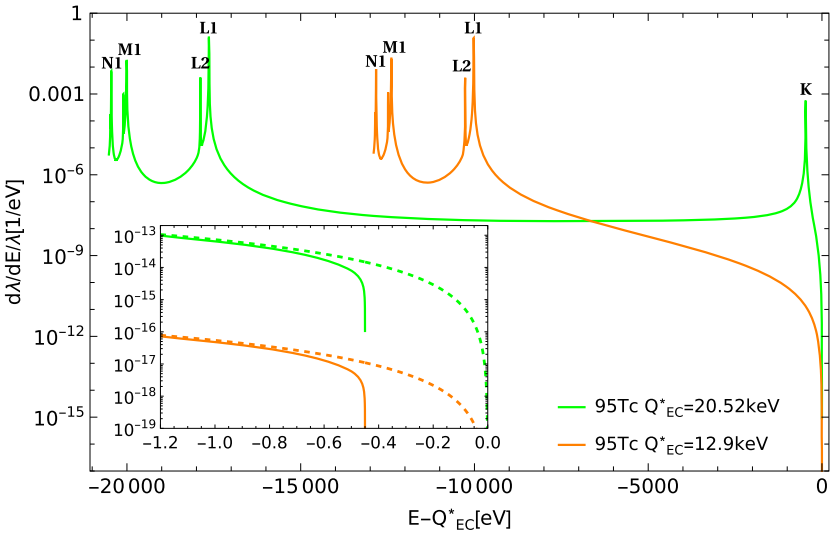
Transition	E^* [keV]	Q^*_{EC} [keV]	Δ_x [keV]
$^{95}\mathrm{Tc}\rightarrow{}^{95}\mathrm{Mo}^*$	1675.40(60)	20.52(61)	0.47(61), K
	1683.0(10)	12.9(10)	10.0(10), L_1
$^{97}\mathrm{Tc}\rightarrow{}^{97}\mathrm{Mo}^*$	320.0(10)	4.8(10)	2.0(10), L_1
$^{113}\mathrm{Sn}\rightarrow{}^{113}\mathrm{In}^*$	1029.650(50)	9.60(20)	5.58(20), L_1
	1024.280(50)	14.97(20)	10.95(20), L_1

- The $^{95}\mathrm{Mo}$ 1683-keV and $^{97}\mathrm{Mo}$ 320-keV spin assignments are uncertain. The displayed $^{97}\mathrm{Tc}$ spectrum assumes an allowed transition.
- The $^{113}\mathrm{In}$ 1024-keV branch is second forbidden non-unique.

*Z. Ge et al., Phys. Lett. B **859**, 139094 (2024); Phys. Rev. C **112**, 035501 (2025); Phys. Rev. C **114**, 035501 (2026)*

^{95}Tc and ^{97}Tc: released-energy spectra

$^{95}\mathrm{Tc} \rightarrow {}^{95}\mathrm{Mo}^*$



$Q^* = 20.52$ and 12.9 keV

*Phys. Lett. B **859**, 139094 (2024)*

$^{97}\mathrm{Tc} \rightarrow {}^{97}\mathrm{Mo}^*$

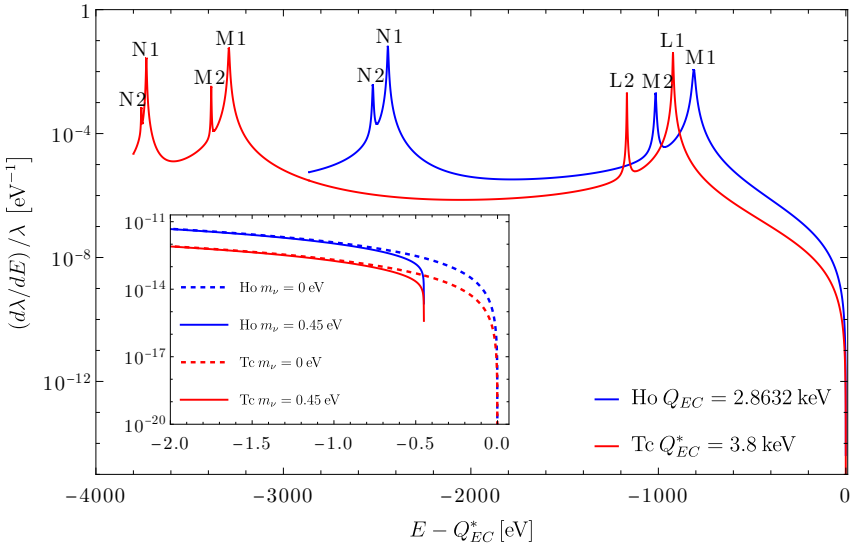


Illustration: $Q^* = 3.8$ keV
(-1σ from $4.8(10)$ keV; allowed assumed)

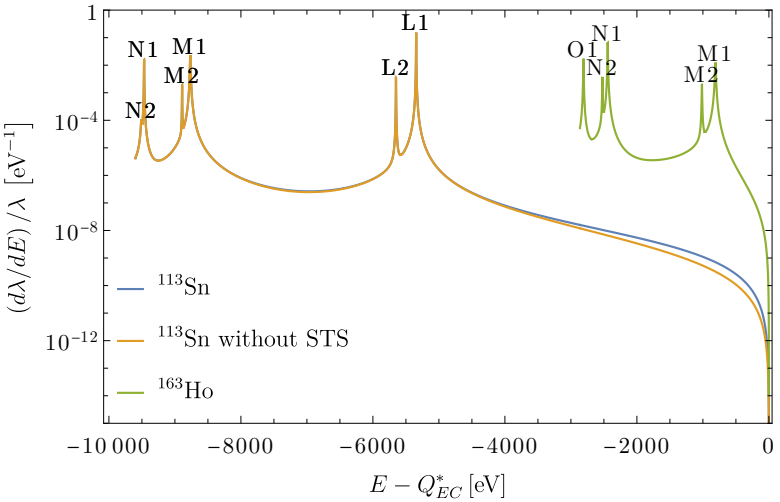
*Phys. Rev. C **112**, 035501 (2025)*

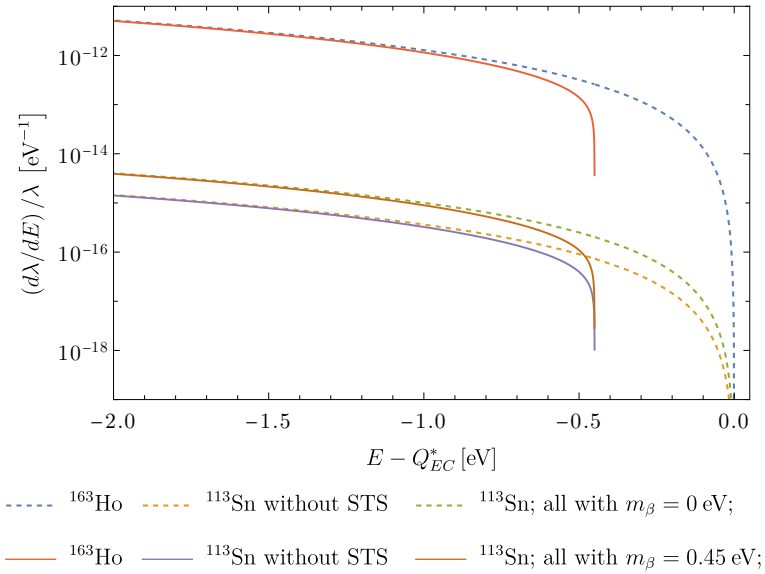
Each spectrum is normalized to its branch.

Absolute yields also depend on the partial half-life.

^{113}Sn: released-energy spectrum

$$^{113}\mathrm{Sn} \longrightarrow {}^{113}\mathrm{In}^{*}(1029.650\ \mathrm{keV}) \quad Q^{*} = 9.60(20)\ \mathrm{keV}$$





$$\Delta_{L_1} = 5.58(20)\ \mathrm{keV}$$

Normalized spectra and their neutrino-mass dependence.

STS: subthreshold-state contribution - Phys. Rev. Lett. **135**, 112502 (2025)

*Z. Ge et al., Phys. Rev. C **114**, 035501 (2026)*

Conclusions

- Final bound–continuum orthogonality is essential for the exchange correction. The $^{63}\mathrm{Ni}$, $^{151}\mathrm{Sm}$ and $^{210}\mathrm{Pb}$ spectra provide experimental tests.

- In $^{187}\mathrm{Re}$, exchange modifies rates and spectral shapes. It must also enter the Kurie definition to preserve massless linearity near the endpoint.

- Low-energy EC transitions to excited states in $^{95}\mathrm{Tc}$, $^{97}\mathrm{Tc}$ and $^{113}\mathrm{Sn}$ motivate further investigation for direct neutrino-mass measurements, but their experimental viability depends on nuclear and atomic properties as well as source and detector constraints.